Engineering 2015, 1(3): 372–377
DOI 10.15302/J-ENG-2015052

Research
Materials Genome—Article

Materials Design on the Origin of Gap States in a High-κ/GaAs Interface

Weichao Wang[1,2], Cheng Gong[1], Ka Xiong[1], Santosh K. C.[1], Robert M. Wallace[1], Kyeongjae Cho[1]*

ABSTRACT Given the demand for constantly scaling microelectronic devices to ever smaller dimensions, a SiO_2 gate dielectric was substituted with a higher dielectric-constant material, $Hf(Zr)O_2$, in order to minimize current leakage through dielectric thin film. However, upon interfacing with high dielectric constant (high-κ) dielectrics, the electron mobility in the conventional Si channel degrades due to Coulomb scattering, surface-roughness scattering, remote-phonon scattering, and dielectric-charge trapping. III-V and Ge are two promising candidates with superior mobility over Si. Nevertheless, $Hf(Zr)O_2$/III-V(Ge) has much more complicated interface bonding than Si-based interfaces. Successful fabrication of a high-quality device critically depends on understanding and engineering the bonding configurations at $Hf(Zr)O_2$/III-V(Ge) interfaces for the optimal design of device interfaces. Thus, an accurate atomic insight into the interface bonding and mechanism of interface gap states formation becomes essential. Here, we utilize first-principle calculations to investigate the interface between HfO_2 and GaAs. Our study shows that As—As dimer bonding, Ga partial oxidation (between 3+ and 1+) and Ga— dangling bonds constitute the major contributions to gap states. These findings provide insightful guidance for optimum interface passivation.

KEYWORDS high-mobility device, high-κ/III-V interface, interfacial gap states, first-principle calculations

1 Introduction

The computational study of electronic device materials has played a critical role in the introduction of new functional materials to meet device-scaling requirements. Conventional field-effect transistor (FET) devices are composed of a Si semiconducting channel, a silicide metal electrode source/drain, and a SiO_2 insulating gate dielectric with a polysilicon metallic gate for the field control of the channel. Over the last decade, Si-based device materials have rapidly been replaced, with high dielectric constant (high-κ) oxides replacing SiO_2 and a metal gate replacing the polysilicon gate [1]. During this rapid process, materials design has played a critical role in guiding potential high-κ dielectric and metal gate material selection from numerous candidate materials [2–5]. Recently, the US government started the Materials Genome Initiative (MGI) with the goal of accelerating the development and commercialization of new materials for advanced engineering system applications [6]. Rather than following the conventional dependence on an empirical trial-and-error approach, the MGI is targeting the introduction of rational materials design during new functional materials development and is intended to achieve an accelerated materials development cycle (significantly shortening the traditional 20-year cycle). It is worthwhile to note that our research work (on another topic) has demonstrated the MGI concept through a commercial product development from a conceptual design within eight years [7–9]. From this perspective, the next step in FET device scaling, the introduction of high-mobility channel materials to replace the Si channel, falls into the category of an MGI problem, and a predictive quantum simulation would provide critical guidance to reduce the development cycle by focusing on the most promising material systems selected by materials design. In this review, we discuss the origin of the trap states formed at the interface between a high-mobility channel and a high-κ gate oxide in order to place this FET device challenge within the MGI framework.

The low interface quality between a high-κ oxide and a III-V channel remains one of the main obstacles in achieving ultra-high-speed semiconductor devices. Despite considerable work on improving the microscopic process, passivation, self-cleaning, and characterization [10–13], the limited understanding of the physical origins of the interface states, trapping the Fermi level in the high-κ oxide/GaAs interface, hinders the progress of a breakthrough in enhancing interface quality. This hindrance is largely due to the complicated interfacial bonding configurations, which vary based on the experimental growth conditions. At the high-κ/GaAs inter-

[1] Department of Materials Science and Engineering, The University of Texas at Dallas, Richardson, TX 75080, USA; [2] College of Electronic Information and Optical Engineering, Nankai University, Tianjin 300071, China
* Correspondence author. E-mail: kjcho@utdallas.edu
Received 23 June 2015; received in revised form 8 September 2015; accepted 14 September 2015

face, Ga (As) may induce various structural disorders such as Ga-(As-)oxides, Ga—Ga (As—As) dimer bonding, Ga— (As—) dangling bonds, and so forth, which might degrade the insulating properties of the interface. As-oxides can be reduced by $(NH_4)_2S$ and NH_4OH and more recently by certain atomic layer deposition (ALD) processes, in a self-cleaning effect [14]. The residual imperfections' impact on the distribution of the gap states therefore becomes critical [15]. Experimentally, the density of interface states (D_{it}) are distributed as three parts, that is, P1, P2, and P3 as shown in Figure 1. The origin of such D_{it} distributions remains an active area of research. For example, there has been a long-term debate [14–16] over whether Ga^{3+} contributes to gap states or not. In addition to Ga 3+, Ga partial charge states, between 3+ and 1+, may occur as oxygen atoms with an unfixed number bond to Ga. These partial charge states may coexist with Ga 3+ and 1+, and may possibly act as a source to generate gap states. Without completely understanding the impact of various Ga charge states on the distribution of the interface gap states, the mechanism of the gap states' distribution is likely incomplete. Moreover, the presence of such oxidation states is likely a sign of a bonding disorder at the interface, which would result in further defect generation such as dangling bonds.

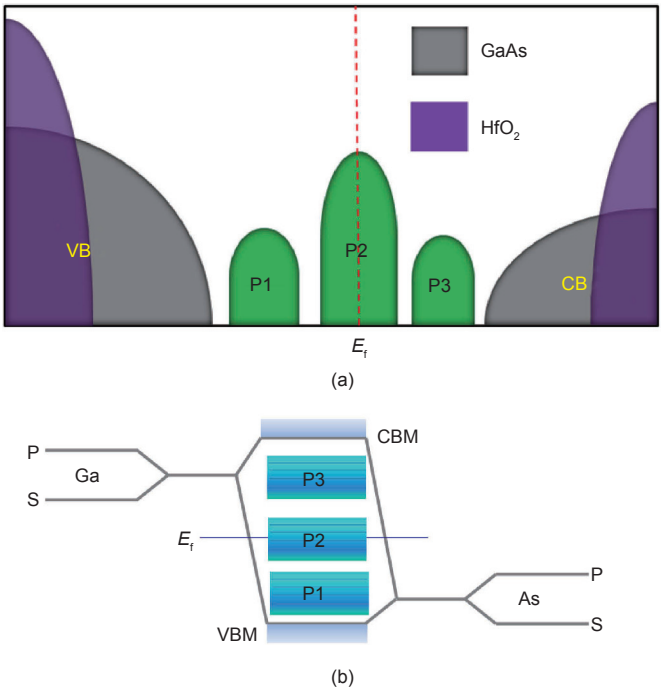

Figure 1. (a) The density of interface states (D_{it}) are distributed as three parts, that is, P1, P2, and P3; (b) defect levels of GaAs with tight binding. VB: valence band; CB: conduction band; VBM: valence band maximum; and CBM: conduction band minimum.

Theoretically speaking, according to an empirical tight-binding analysis in bulk GaAs, as shown in Figure 1(b), Ga— (As—) dangling bonds generate conducting (valence) edge states (VB: P1 and CB: P3). As—As (Ga—Ga) dimers and Ga (As) antisites produce mid-gap states—P2 in Figure 1(b) [17]. Nevertheless, this model provides insufficient insight into the origin of gap states in the GaAs/oxide interface, because interfacial bonding is not considered. In fact, at a high-κ/GaAs interface, high-κ oxides such as HfO_2 have ionic bonding without a fixed atomic coordination and fixed bond angles, leading to various charge states of interfacial Ga and As. Such charge states correspond to different types of unsaturated Ga (As) bonds, generating gap states.

Intrinsically, it is difficult to achieve an electronically abrupt high-κ/GaAs interface without any structural imperfections because: ① the GaAs (001) surface is polar, and ② Ga is tri-valent and As is penta-valent. Each Ga—As bond has 0.75 electron from Ga and 1.25 electrons from As, which makes electron-counting rules, and Ga (As) covalent bonding angle and direction rigid requirements [18] hard to satisfy. This situation implies that the partially charged Ga (As) bonding leads to the interface gap states. Recently, Robertson et al. [19] proposed that (001)-oriented GaAs/HfO_2 interfaces be modeled by 1 × 1 unit cells of a GaAs and HfO_2 surface, and concluded that an insulating interface is possibly obtained by substituting one O on an As site in the GaAs layer below. However, this interface model contains a large interfacial planar strain (> 10 %) originating from the large lattice mismatch between HfO_2 (5.07 Å) and GaAs (5.65 Å), which makes the model interface problematic.

On the unreconstructed GaAs surface terminated with Ga (As), the atoms form a square array. Each surface Ga (As) has two partially occupied dangling bonds pointing out of the surface. Neither Hf nor O can directly passivate Ga— (As—) dangling bonds based on the Ga (As)—O covalent bonding rigid requirement, unless a large planar strain is applied on the interface, which is not realistic in practice. An alternative approach is to systematically model the effect of oxygen incorporation at the interface [20]. The detection of such bonding and the corresponding oxidation state from high-κ dielectric processes or surface treatments is well-documented experimentally [21].

2 Results and discussion

One example is the interface model labeled O10, shown in Figure 2, in which each oxygen layer has ten oxygen atoms and each Ga (As) layer has four Ga (As) atoms. Thus, five oxygen atoms are required on the HfO_2 surface in order to form an insulating HfO_2 surface. There are eight Ga— dangling bonds at the GaAs surface, which need to be passivated by three oxygen atoms. Consequently, interface O10 ends up with two excess oxygen atoms at the interface. These two excess oxygen atoms are removed to generate a neutral interface. Although the overall interface is charge neutral, the

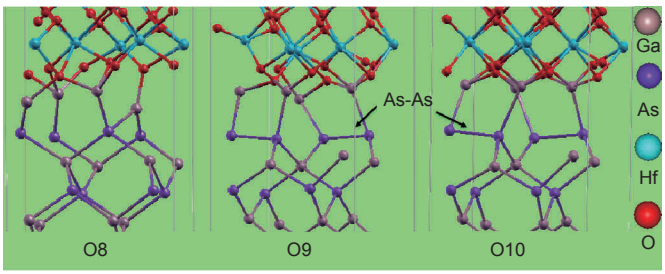

Figure 2. Side views of (100) interface O8, O9, and O10. The Ga, As, Hf, and O atoms are depicted by grey, purple, light blue, and red balls, respectively [20].

three oxygen atoms are not likely to assign 1.25 electrons uniformly to each Ga bond, so the situation inevitably creates gap states, trapping the Fermi level. In addition, another neutral interface could be built after removing two interfacial Ga atoms and five oxygen atoms from the interface, after which both the GaAs surface and the HfO_2 would be insulating. However, this second interface would be unstable due to a much lower degree of Ga—O bonding than in the interface with full-oxygen termination.

One important parameter influencing interface stability is the external oxygen chemical potential, which controls interfacial oxidation and essentially governs interface stability. For example, for the state-of-the-art ALD, interface stability strongly relies on the oxidant (O_3, O_2, and H_2O [22, 23]) concentration. In order to explore external oxygen chemical potential impact at the interfacial oxygen concentration, one to seven oxygen atoms are removed from the interface sequentially [20], and the formation energy of the interfaces as a function of the oxygen chemical potential, constrained by O_2 and HfO_2, is applied (Figure 3). This exploration reveals that an interface with nine interfacial oxygen atoms (labeled O9/Ga4 in Figure 2) has the lowest formation energy within a large oxygen chemical potential range (~ 49.0%). In addition, we find that the neutral charged interface with eight interfacial oxygen atoms is only stable within 21.6% of the whole growth condition range. Another neutral charged interface with two Ga and five O atoms at the interface is apparently not stable within the whole oxygen chemical potential range. On the contrary, the ~ 49.0% growth condition produces a non-neutral charged interface, O9. This observation explains why atomically and electronically abrupt interfaces are not likely to occur spontaneously.

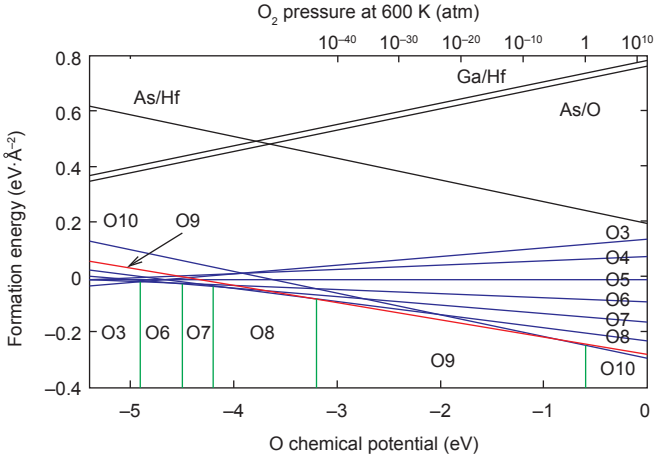

Figure 3. Interface formation energies of various interfacial structures as a function of oxygen chemical potential. Ga—O bonding: labeled as O3 to O10 based on the number of interfacial O atoms; As—Hf bonding: As/Hf; As—O bonding: As/O; and Ga—Hf bonding: Ga/Hf [20]. 1 atm = 101.325 kPa.

Based on their oxygen-rich conditions, O8, O9, and O10 interfaces are the most relevant in realistic interfaces where oxide formation is not carefully controlled, and are thus presented in Figure 2. For the O9 interface, the most stable model within a large oxygen chemical potential range, one of the Ga—As bonds between the second (As) and third (Ga) atomic layers of GaAs is broken, and the optimized interface structure spontaneously forms a Ga— dangling bond and two As—As dimer pairs two layers and one layer away, respectively, from the Ga—O interface bonds. A similar effect is found for the O10 interface. Interestingly, the O8 interface has the least "wrong bonding" (i.e., As—As and Ga— dangling bonds) due to the neutral charge at the interface. To further check Ga and As charge states, Bader charge [24] calculations are performed, as shown in Figure 4(a) and (b). For the O10 model interface, interfacial Ga charge states are close to 3+. As oxygen is depleted from the O10 interface, more partial charge states of Ga begin to occur for the O9 and O8 models, as shown in Figure 4(a). For As charge states, As—As dimer charge states are found for the O9 and O10 interfaces, as shown in Figure 4(b).

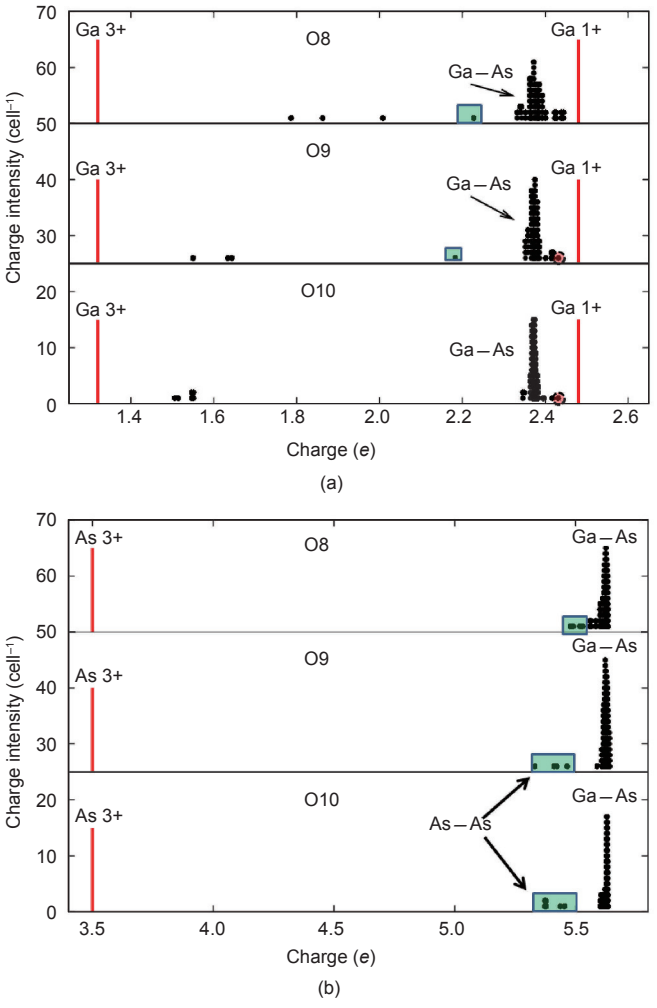

Figure 4. The charge distribution of bulk and interfacial (a) Ga and (b) As for interfaces O8, O9, and O10.

Figure 5 shows the bulk GaAs (grey color) and interface density of states (DOS) for the O8/Ga4, O9/Ga4, and O10/Ga4 models with a Heyd-Scuseria-Ernzerhof (HSE) hybrid functional. The bulk DOS is represented by the Ga (As) atoms far away from the interface. Within the bulk GaAs gap region, three interface states are found, causing Fermi-level pinning. In order to explore the origin of the gap states, the partial charge distribution within the gap region is displayed

in the inset diagram of Figure 5. As O9/Ga4 shows the most stability within a large growth condition of oxygen chemical potential, we examine the charge states of interfacial Ga and As atoms (Figure 4). We label the four interfacial Ga atoms G1, G2, G3, and G4 with the charge states 1.64*e*, 1.63*e*, 2.23*e*, and 1.63*e*, respectively. The partial charge clearly indicates that the interface gap states P1, P2, and P3 arise from Ga (G2) partial oxidation, Ga— dangling bonds, and As—As dimers, respectively. Ga (G1, G3, and G4) 3+ does not directly contribute to gap states.

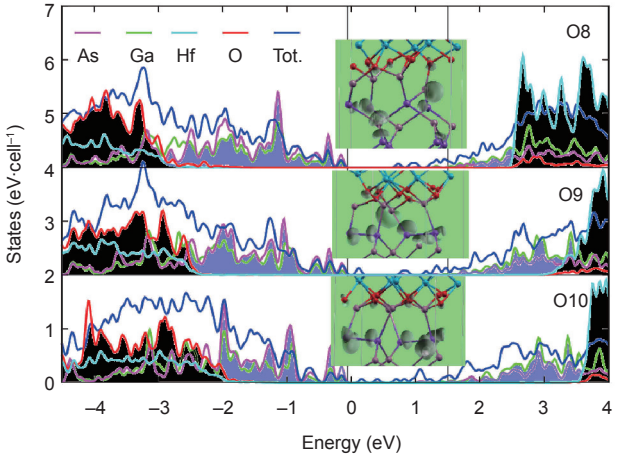

Figure 5. The DOS of bulk GaAs (grey zone) and interfaces O8, O9, and O10. Bulk DOS is magnified by two times and the interface DOS is normalized. Interface states within the bulk GaAs gap region are filled with pink color. The VBM and the CBM are represented by the VB and the CB edge, respectively. The Fermi level is set at 0 eV. The inset figure shows the partial charge distribution within the gap region. The O8, O9, and O10 contour spacing is 4.0×10^{-2} eV·Å^{-3}.

Essentially, interfacial oxygen attracts electrons from adjacent Ga atoms driven by the strong oxygen electronegativity. As a result, Ga charge states such as Ga 3+, Ga 1+ and some intermediate states form. As atoms located beneath interfacial Ga offer more electrons to their upper bonding partners than to their lower bonding neighbors. To compensate for the As charge loss, As—As dimers form. We find that the formation of Ga— dangling bonds and As—As dimers strongly depends on interfacial Ga charge states. Specifically, the big-charge-loss-induced formation of Ga 3+ drives an As big charge loss as well, and thus As forms As—As dimers. Experimentally, the coexistence of Ga 3+ and As—As dimers makes it difficult to identify the real contributor to gap states. Hypothetically, interfacial Ga charge states reduce to 1+ (Ga_2O), which donates less charge than 3+; since interfacial As, As—As dimers, and Ga— dangling bonds would also be removed, the gap states are expected to be eliminated accordingly [25, 26]. This finding sheds a bright light on efficient interface passivation mechanisms.

The use of amorphous Si (a-Si) appears to be an effective passivation scheme. With the presence of a-Si at the interface, Si donates charges to interfacial Ga and transforms Ga partial oxidation states to 1+; meanwhile, As—As dimers obtain enough charge from the Si to break the dimer bonds [27].

In addition to the interface thermal stability and the DOS, the injection barrier is another critical parameter of a semiconductor device [28], and is represented by the band offsets between the VB edges of the gate oxide and semiconductor. For device applications, the injection barrier requires greater than 1.0 eV in order to prevent electrons from entering the oxide CB, through which carriers can cross the gate oxide [29].

The valence band offset (VBO) is accurately predicted using the reference potential method [30, 31]. For the interface model O9, the VBOs are 1.81 eV. As a comparison, the experimental data show diverse values of VBO: 2.00 eV [32], 2.10 eV [33], and 2.85 eV [34]. Robertson and Falabretti used the charge neutral level (CNL) method without considering the observed interface bonding in order to predict a value of 3.00 eV [35]. These findings confirm the promising injection barrier between HfO_2 and GaAs.

In summary, we apply density functional theory (DFT) in order to find the origin of HfO_2/GaAs interface gap states; that is, As—As dimers, Ga partial oxidation states, and Ga— dangling bonds inducing gap states. Ga 3+ does not directly generate any gap states. In addition, band offset results illustrate that the GaAs/HfO_2 interface is a good candidate to prevent carrier injection through oxide thin film.

3 Method

A 10 Å vacuum region was used in order to avoid interactions between the top and bottom atoms in the periodic slab images. The bottom Ga atoms are passivated by pseudohydrogen (with 1.25 valence electrons) to mimic As—bulk bonds. The top layer of HfO_2 is initially terminated by ten oxygen atoms in the unit cell; half of these are removed in order to generate an insulating HfO_2 surface. The applied passivation of the top (HfO_2) and bottom (GaAs) surfaces guarantees that the top and bottom surface states are removed and all the calculated gap states originate from the interface. The GaAs slab is 27.16 Å thick with ten layers of Ga and nine layers of As, while the HfO_2 slab is 13.42 Å thick with five layers of Hf and six layers of O. This slab thickness is big enough to reduce the quantum size effect [36, 37]. The conjugate gradient (CG) was used to perform structural optimization with only the bottom of the passivated GaAs layers fixed. The force accuracy reaches 0.01 eV·Å^{-1}.

The nature of interface electronic states depends strongly on the details of the atomic structure and bonding at the interface, signifying the importance of an accurate interface model. In the process of building a convincing theoretical model for an HfO_2/GaAs interface, several issues must be considered: First, the lattice mismatch needs to be accommodated by the strain; second, the interface should be thermally stable and realistic; third, experimental information must be taken into account and must validate the theoretical model; fourth, the DFT limit of searching the global minimum energy for a relaxed interface needs to be reduced as much as possible.

In this work, we consider the interface between cubic HfO_2 and GaAs. Although HfO_2 exists in cubic, tetragonal, and monoclinic phases, these all have very similar local ionic bonding characteristics, and the atomic structures are closely

related [38]. Cubic HfO_2 is allowed to change into lower energy structures during the atomic structure optimization. Furthermore, the conclusions from the current analysis would be applicable to other phases, because the key requirement is valence satisfaction, which depends on the local bonding configuration rather than on long-range crystalline symmetry. We use a periodic slab model with Ga—O bonds at the interface (formed by Ga-terminated GaAs and O-terminated HfO_2 surfaces), which is supported by experimental data [39, 40]. The (001)-oriented HfO_2 surface was compressed by ~ 0.3% and rotated counter-clockwise by 28.04°, that is, 28.04 = 45 – 16.96, to match the GaAs (001) surface (Figure 6). The CG [41] method was applied for the atomic structure optimization. Because the CG method would only lead to the local minimum, it is possible that the optimized structures are metastable interface structures. To investigate diverse interface structures formed between the GaAs and HfO_2 surfaces, the HfO_2 slab was moved in the x and xy directions relative to the GaAs slab, and the local energy minimum structures were obtained as a function of the relative shift. The interface formation energy was lowered by 1.5 eV at the shift of 1.0 Å along the xy direction, resulting in the lowest total energy. We use this minimum energy interface structure as the initial structure and perform a full relaxation.

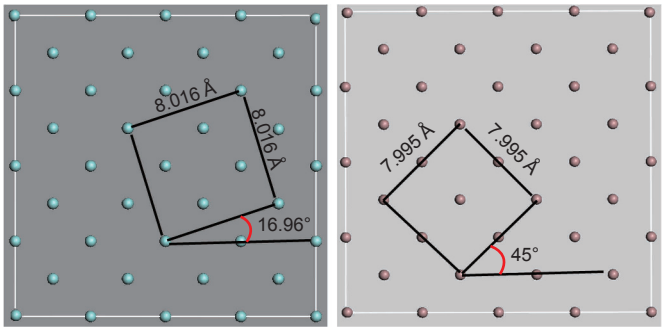

Figure 6. (a) The Hf monolayer for HfO_2 bulk normal to (001) direction; (b) the Ga monolayer for GaAs (001) bulk normal to (001) direction. Bright green atoms are Hf and grey atoms are Ga [20].

For high-level electronic structure calculations, HSE [42], which produces band gaps and equilibrium lattice parameters that are in much better agreement with experimental results than local density approximations (LDA) or generalized gradient approximations (GGA) [43, 44], was applied in order to overcome the well-known DFT limitation [40, 41]: band gap underestimation. A 25% Hartree-Fock exchange potential was incorporated into a Perdew-Burke-Ernzerhof (PBE) [45] potential, resulting in a 1.40 eV gap being obtained; this result is close enough to the experimental value of 1.42 eV [46].

Acknowledgements

This work was supported by the National Natural Science Foundation of China (11304161, 11104148, and 51171082), the Tianjin Natural Science Foundation (13JCYBJC41100 and 14JCZDJC37700), the National Basic Research Program of China (973 Program) (2014CB931703), Specialized Research Fund for the Doctoral Program of Higher Education (20110031110034), and the Fundamental Research Funds for the Central Universities. Kyeongjae Cho was supported by the Global Frontier Center for Multiscale Energy Systems at Seoul National University in Korea. We thank the technology support from the Texas Advanced Computing Center (TACC) at the University of Texas at Austin (http://www.tacc.utexas.edu) for providing computing resources.

Compliance with ethics guidelines

Weichao Wang, Cheng Gong, Ka Xiong, Santosh K. C., Robert M. Wallace, and Kyeongjae Cho declare that they have no conflict of interest or financial conflicts to disclose.

References

1. J. Robertson, R. M. Wallace. High-k materials and metal gates for CMOS applications. *Mat. Sci. Eng. R.*, 2015, 88: 1–41
2. K. Cho. First-principles modeling of high-k gate dielectric materials. *Comp. Mater. Sci.*, 2002, 23(1–4): 43–47
3. M. Haverty, A. Kawamoto, K. Cho, R. Dutton. First-principles study of transition-metal aluminates as high-k gate dielectrics. *Appl. Phys. Lett.*, 2002, 80(15): 2669–2671
4. S. Park, L. Colombo, Y. Nishi, K. Cho. *Ab initio* study of metal gate electrode work function. *Appl. Phys. Lett.*, 2005, 86(7): 073118
5. J. H. Ha, P. C. McIntyre, K. Cho. First principles study of the HfO_2/SiO_2 interface: Application to high-k gate structures. *J. Appl. Phys.*, 2007, 101(3): 033706
6. The White House. About the Materials Genome Initiative. https://www.whitehouse.gov/mgi
7. B. Lee, K. Cho. Extended embedded-atom method for platinum nanoparticles. *Surf. Sci.*, 2006, 600(10): 1982–1990
8. X. Hao, et al. Experimental and theoretical study of CO oxidation on PdAu catalysts with NO pulse effects. *Top. Catal.*, 2009, 52(13–20): 1946–1950
9. B. Shan, et al. First-principles-based embedded atom method for PdAu nanoparticles. *Phys. Rev. B*, 2009, 80(3): 035404
10. M. J. Hale, S. I. Yi, J. Z. Sexton, A. C. Kummel, M. Passlack. Scanning tunneling microscopy and spectroscopy of gallium oxide deposition and oxidation on GaAs(001)-c(2×8)/(2×4). *J. Chem. Phys.*, 2003, 119(13): 6719–6728
11. D. L. Winn, M. J. Hale, T. J. Grassman, A. C. Kummel, R. Droopad, M. Passlack. Direct and indirect causes of Fermi level pinning at the SiO/GaAs interface. *J. Chem. Phys.*, 2007, 126(8): 084703
12. M. Passlack, R. Droopad, P. Fejes, L. Wang. Electrical properties of Ga_2O_3/GaAs interfaces and GdGaO dielectrics in GaAs-based MOSFETs. *IEEE Electr. Device L.*, 2009, 30(1): 2–4
13. C. L. Hinkle, et al. Comparison of *n*-type and *p*-type GaAs oxide growth and its effects on frequency dispersion characteristics. *Appl. Phys. Lett.*, 2008, 93(11): 113506
14. C. L. Hinkle, M. Milojevic, E. M. Vogel, R. M. Wallace. The significance of core-level electron binding energies on the proper analysis of InGaAs interfacial bonding. *Appl. Phys. Lett.*, 2009, 95(15): 151905
15. R. V. Galatage, et al. Accumulation capacitance frequency dispersion of III-V metal-insulator-semiconductor devices due to disorder induced gap states. *J. Appl. Phys.*, 2014, 116(1): 014504
16. M. Passlack, M. Hong, J. P. Mannaerts, S. N. G. Chu, R. L. Opila, N. Moriya. In-situ Ga_2O_3 process for GaAs inversion/accumulation device and surface

passivation applications. In: *1995 International Electron Devices Meeting*. Piscataway, NJ: IEEE, 1995: 383–386

17. E. P. O'Reilly, J. Robertson. Electronic structure of amorphous III-V and II-VI compound semiconductors and their defects. *Phys. Rev. B Condens. Matter*, 1986, 34(12): 8684–8695
18. P. W. Peacock, J. Robertson. Bonding, energies, and band offsets of Si-ZrO_2 and HfO_2 gate oxide interfaces. *Phys. Rev. Lett.*, 2004, 92(5): 057601
19. J. Robertson, L. Lin. Fermi level pinning in Si, Ge and GaAs systems—MIGS or defects? In: *2009 International Electron Devices Meeting*. Piscataway, NJ: IEEE, 2009: 119
20. W. Wang, K. Xiong, R. M. Wallace, K. Cho. Impact of interfacial oxygen content on bonding, stability, band offsets, and interface states of GaAs:HfO_2 interfaces. *J. Phys. Chem. C*, 2010, 114(51): 22610–22618
21. C. L. Hinkle, E. M. Vogel, P. D. Ye, R. M. Wallace. Interfacial chemistry of oxides on $In_xGa_{(1-x)}As$ and implications for MOSFET applications. *Curr. Opin. Solid St. M.*, 2011, 15(5): 188–207
22. K. Kukli, M. Ritala, T. Sajavaara, J. Keinonen, M. Leskelä. Atomic layer deposition of hafnium dioxide films from hafnium tetrakis(ethylmethylamide) and water. *Chem. Vapor. Depos.*, 2002, 8(5): 199–204
23. S. Keun Kim, C. Seong Hwang, S. H. Ko Park, S. Jin Yun. Comparison between ZnO films grown by atomic layer deposition using H_2O or O_3 as oxidant. *Thin Solid Films*, 2005, 478(1–2): 103–108
24. G. Henkelman, A. Arnaldsson, H. Jónsson. A fast and robust algorithm for Bader decomposition of charge density. *Comp. Mater. Sci.*, 2006, 36(3): 354–360
25. J. Robertson. Model of interface states at III-V oxide interfaces. *Appl. Phys. Lett.*, 2009, 94(15): 152104
26. W. Wang, G. Lee, M. Huang, R. M. Wallace, K. Cho. First-principles study of GaAs (001)-β2 (2 × 4) surface oxidation and passivation with H, Cl, S, F, and GaO. *J. Appl. Phys.*, 2010, 107(10): 103720
27. W. Wang, K. Xiong, C. Gong, R. M. Wallace, K. Cho. Si passivation effects on atomic bonding and electronic properties at HfO_2/GaAs interface: A first-principles study. *J. Appl. Phys.*, 2011, 109(6): 063704
28. J. Robertson. Band offsets of wide-band-gap oxides and implications for future electronic devices. *J. Vac. Sci. Technol. B*, 2000, 18(3): 1785–1791
29. G. D. Wilk, R. M. Wallace, J. M. Anthony. High-κ gate dielectrics: Current status and materials properties considerations. *J. Appl. Phys.*, 2001, 89(10): 5243–5275
30. C. G. van de Walle, R. M. Martin. Theoretical study of band offsets at semiconductor interfaces. *Phys. Rev. B Condens. Matter*, 1987, 35(15): 8154–8165
31. H. M. Al-Allak, S. J. Clark. Valence-band offset of the lattice-matched β-$FeSi_2$(100)/Si(001) heterostructure. *Phys. Rev. B*, 2001, 63(3): 033311
32. V. V. Afanas'ev, et al. Energy barriers at interfaces of (100)GaAs with atomic layer deposited Al_2O_3 and HfO_2. *Appl. Phys. Lett.*, 2008, 93(21): 212104
33. G. Seguini, M. Perego, S. Spiga, M. Fanciulli, A. Dimoulas. Conduction band offset of HfO_2 on GaAs. *Appl. Phys. Lett.*, 2007, 91(19): 192902
34. G. K. Dalapati, H. J. Oh, S. J. Lee, A. Sridhara, A. S. W. Wong, D. Chi. Energy-band alignments of HfO_2 on *p*-GaAs substrates. *Appl. Phys. Lett.*, 2008, 92(4): 042120
35. J. Robertson, B. Falabretti. Band offsets of high *K* gate oxides on III-V semiconductors. *J. Appl. Phys.*, 2006, 100(1): 014111
36. A. G. Cullis, L. T. Canham. Visible light emission due to quantum size effects in highly porous crystalline silicon. *Nature*, 1991, 353(6342): 335–338
37. V. Lehmann, U. Gösele. Porous silicon formation: A quantum wire effect. *Appl. Phys. Lett.*, 1991, 58(8): 856–858
38. J. Zhu, Z. G. Liu. Structure and dielectric properties of ultra-thin ZrO_2 films for high-k gate dielectric application prepared by pulsed laser deposition. *Appl. Phys. A-Mater.*, 2004, 78(5): 741–744
39. C. L. Hinkle, et al. GaAs interfacial self-cleaning by atomic layer deposition. *Appl. Phys. Lett.*, 2008, 92(7): 071901
40. C. L. Hinkle, et al. Detection of Ga suboxides and their impact on III-V passivation and Fermi-level pinning. *Appl. Phys. Lett.*, 2009, 94(16): 162101
41. W. H. Press, B. P. Flannery, S. A. Teukolsky, W. T. Vetterling. *Numerical Recipes: The Art of Scientific Computing*. New York: Cambridge University Press, 1986
42. J. P. Perdew, M. Ernzerhof, K. Burke. Rationale for mixing exact exchange with density functional approximations. *J. Chem. Phys.*, 1996, 105(22): 9982–9985
43. P. Hohenberg, W. Kohn. Inhomogeneous electron gas. *Phys. Rev.*, 1964, 136(3B): B864–B871
44. W. Kohn, L. J. Sham. Self-consistent equations including exchange and correlation effects. *Phys. Rev.*, 1965, 140(4A): A1133–A1138
45. J. P. Perdew, K. Burke, M. Ernzerhof. Generalized gradient approximation made simple. *Phys. Rev. Lett.*, 1996, 77(18): 3865–3868
46. L. C. West, S. J. Eglash. First observation of an extremely large-dipole infrared transition within the conduction band of a GaAs quantum well. *Appl. Phys. Lett.*, 1985, 46(12): 1156–1158